Focus Section: Statistical Seismology and Probabilistic Earthquake Forecasting

Improvements and Heterogeneities of the Global Centroid Moment Tensor Catalog

Álvaro González*[1,2]

Abstract

Earthquake catalogs are heterogeneous, especially those developed over long time spans. Changes in seismological monitoring, which provides the records on which these catalogs are based, are common. Typically, instruments and networks become more sensitive over time, allowing for the detection and characterization of smaller earthquakes. In pursuit of improvement, new methods for routine data analysis are occasionally introduced, modifying the procedures for catalog compilation. The resulting heterogeneities may not be evident to users, but they should be unveiled and considered in any application of the catalog, especially in statistical seismology, which analyzes large earthquake data sets. The Global Centroid Moment Tensor catalog is considered the most homogeneous database of global seismicity. However, a detailed analysis of its heterogeneities has been lacking. This work reviews changes in the catalog's development from 1976 to 2023 and reveals how these have caused improvements and heterogeneities in the resulting data. Several periods are distinguished, separated by milestones in the methods employed for moment tensor inversion and catalog compilation, as well as by the advent of global broadband monitoring in 2004. These changes are shown to have caused variations in the catalog's completeness and in the determinations of centroid depths, scalar seismic moments, and moment tensors. The magnitude of completeness is measured here in detail, both temporally and spatially. It has decreased over the years and shows spatial variations within each period, correlated to regional differences in network monitoring and compilation biases. Moment tensor determinations have been significantly different since 2004, resulting in a different frequency distribution of rake angles and a different dependence of the double-couple component as a function of rake. This work is expected to benefit all future uses of the catalog, enabling better characterization of seismicity properties and improved building and testing of models for earthquake occurrence.

Cite this article as González, Á. (2024). Improvements and Heterogeneities of the Global Centroid Moment Tensor Catalog, *Seismol. Res. Lett.* **95**, 3566–3578, doi: 10.1785/0220240272.

Supplemental Material

Introduction

The Global Centroid Moment Tensor (Global CMT) catalog (Dziewonski *et al.*, 1981; Ekström *et al.*, 2012; Ekström, 2015; Ekström and Nettles, 2015) provides estimates of the focal mechanism, scalar seismic moment (M_0), and centroid location for major earthquakes worldwide and has become one of the most used databases in seismology. Apart from offering global insights on Earth's seismicity and seismotectonics (e.g., Ekström, 2015), it has allowed systematic analyses of earthquake size distributions (e.g., Yoder *et al.*, 2012; Kagan and Jackson, 2016; Serra and Corral, 2017; Corral and González, 2019), thanks to M_0 being a physically meaningful and consistent size measurement reliable up to the largest earthquakes (e.g., Deichmann, 2018). In contrast, many earthquake catalogs contain a mixture of nonequivalent magnitude scales, which complicates such analyses (e.g., Di Giacomo and Storchak, 2016; González, 2017; Herrmann and Marzocchi, 2021). The Global CMT catalog has also enabled showing how the earthquake size distribution depends on the faulting style (Schorlemmer *et al.*, 2005; Petruccelli *et al.*, 2018, 2019). And it has been used to identify that the latter is correlated to the double-couple component of the focal mechanism (Zaccagnino and Doglioni, 2022). Moreover, it is being employed as a benchmark catalog for developing and testing forecasts of earthquake rates (e.g., Kagan and Jackson, 2011; Bird *et al.*, 2015) and focal mechanisms (e.g., Kagan and Jackson, 2014; Taroni and Selva, 2021). And, in turn, it is a major data source for other databases, such as the

1. CRM Centre de Recerca Matemàtica, Barcelona, Spain, https://orcid.org/0000-0002-9300-4283 (ÁG); 2. GFZ German Research Centre for Geosciences, Potsdam, Germany

*Corresponding author: agonzalez@crm.cat, alvarog@gfz-potsdam.de

International Seismological Centre (ISC) Bulletin (Lentas *et al.*, 2019; Di Giacomo *et al.*, 2021; International Seismological Centre, 2024), the International Seismological Centre-Global Earthquake Model (ISC-GEM) catalog (Di Giacomo *et al.*, 2015, 2018; Lee and Engdahl, 2015) or diverse regional earthquake compilations (e.g., Mueller, 2019).

As is typical for most catalogs, heterogeneities and temporal changes are to be expected on it, given the methodological improvements for data analysis introduced over its development (e.g., Ekström *et al.*, 2012), and the expansion of the seismological networks which provided the records used for compiling the catalog. For example, only 10–20 stations contributed globally with digital data to the catalog in the early 1980s, but more than 200 stations did in 2012 (Ekström and Nettles, 2015).

A crucial issue is how complete the catalog is. Its compilers acknowledge an improvement from an overall magnitude of completeness (M_c) from $M_c \sim 5.4$ during 1976–2003 to $M_c \sim 5.0$ for 2004–2013 (Ekström and Nettles, 2015), but these estimates are optimistic compared to more detailed ones. Higher values of M_c were noted by Kagan (2003), who considered its temporal variations, but not the spatial ones, and by Woessner and Wiemer (2005) and Petruccelli *et al.* (2019), who mapped its spatial variations but disregarded temporal ones. Di Giacomo *et al.* (2021) compared M_c of this catalog to others, but only in specific regions and periods. So an updated, comprehensive appraisal, considering both the spatial and temporal variations of M_c, would be indeed necessary for the catalog users.

This contribution first identifies the major eras in which the catalog may be divided, based on milestones in its development. Considering these periods, M_c is then determined in unprecedented temporal and spatial detail. I next show how the resulting heterogeneities alter the spatial pattern of centroid depths, the statistical distribution of rakes (which determine the faulting styles), and the fraction of the double-couple component as a function of rake.

I will not overlap with other catalog issues already discussed in detail elsewhere, for example as follows. Agnew (2015) noted apparent magnitude heterogeneities in the catalog. Uncertainties in the seismic moment tensors were analyzed, for example, by Rösler *et al.* (2021). Finally, location errors of the centroids were discussed, for example, by Ferreira and Woodhouse (2006), Hjörleifsdóttir and Ekström (2010), Morales-Yáñez *et al.* (2020), Wimpenny and Watson (2021), and Sawade *et al.* (2022).

Catalog History: Temporal Heterogeneities in the Catalog Compilation

Here, I will analyze the Global CMT catalog (see Data and Resources) for the 48 full years published so far (1976–2023), which include a total of 64,879 earthquakes. See supplemental Videos S1 and S2, available to this article, for animated globes (blank and with the epicentroid map, respectively). Moment magnitudes (M_w) were calculated from the reported M_0 (measured in dyn · cm) as $M_w = (2/3)(\log M_0 - 16.1)$. This equation, also used in the web searches of the catalog since February 2006, avoids rounding issues (see Bormann, 2015), which may arise when applying the original formulae by Kanamori (1977) and Hanks and Kanamori (1979).

To analyze the evolution and heterogeneities of an earthquake catalog, it is necessary to separate eras with different techniques for data processing, earthquake location, or magnitude determination, or according to the development of the network contributing data for the catalog compilation (e.g., Hutton *et al.*, 2010; González, 2017). So, a first step is to identify the milestones that separate such periods.

For the Global CMT catalog, I will initially tell apart four eras (Fig. 1), which are quite apparent when considering the global rate of earthquakes reported in the catalog (increasing as the methods and networks improved) and the procedures for centroid depth determination. They are also based on improvements of the routine CMT analysis for the catalog (Ekström and Nettles, 2015) and on a major milestone in the development of the Global Seismographic Network, which is used as a major data source for the catalog, complemented by other, global and regional networks (Ekström *et al.*, 2012; Ekström and Nettles, 2015). Further catalog heterogeneities may be unveiled using scatterplots of magnitude versus time, which were already explored by Agnew (2015, his fig. 8).

Transient, actual, increases in the global seismicity rates were due to the high productivity of the aftershock sequences of the great earthquakes of Sumatra–Andaman (26 December 2004; see Lay *et al.*, 2005) and Tohoku-Oki (11 March 2011). But the general trend (Fig. 1a) is expected to evidence the improvements in the seismic monitoring and data analysis over time, which allowed including more small earthquakes in the catalog. This is made clear by plotting separately the cumulative number of events with magnitude not larger than the current median (Fig. 1a).

Moment tensor inversion using long-period waves, as used for the CMT catalog, cannot resolve the depth of shallow seismic sources (e.g., Hejrani and Tkalčić, 2020). For this reason, shallow earthquakes have been assigned a minimum, fixed depth, in the catalog, which has changed over time. Such changes may be missed by the catalog users, since the most recent catalog descriptions (Ekström *et al.*, 2012; Ekström and Nettles, 2015) only mention the value used since 2004. Other centroid depths could not be resolved either and are fixed at the hypocentral depth or at a value considered suitable by the analyst, considering the regional seismicity (Ekström and Nettles, 2015). Fixed depths are suitably flagged in the catalog files, indicating whether they were not inverted for (so fixed in strict sense) or whether they were based on the modeling of broadband *P* waveforms (body waves, Fig. 1b).

The eras and their rationale would be as follows:

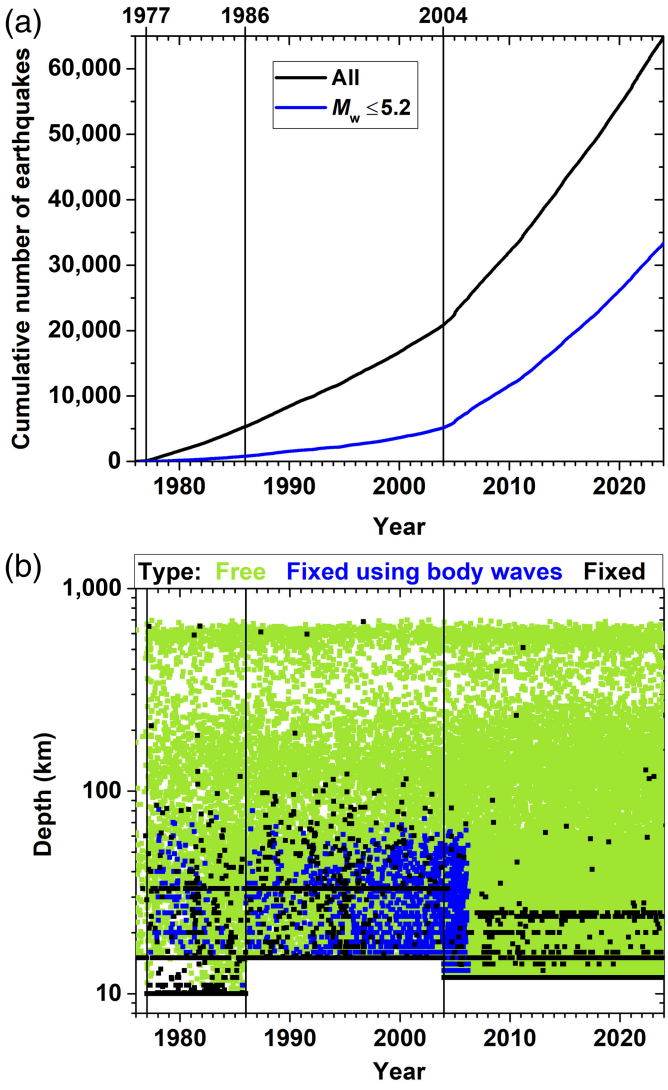

Figure 1. Eras distinguished in the Global Centroid Moment Tensor (Global CMT) catalog, separated by the beginning of the years 1977, 1986, and 2004 (marked). (a) Cumulative number of earthquakes, for all magnitudes or for moment magnitude $M_w \leq 5.2$ (median magnitude as of the end of 2023 in the catalog). (b) Centroid depths and their determination type. Note that in panel (b) the vertical scale is logarithmic, to enhance the differences in the minimum depth used during different eras (10, 12, or 15 km). The color version of this figure is available only in the electronic edition.

1976

The catalog for this year (only 108 earthquakes) was published by Ekström and Nettles (1997), using the procedures then in practice, such as a fixed depth of 15 km for shallow centroids.

1977–1985

After the initial CMT method was published (Dziewonski *et al.*, 1981), the catalog compilation started in 1982 at Harvard University, as the Harvard CMT project, led by Adam Dziewonski. During 1977–1985, an average of 540 earthquakes per year were reported (almost a fivefold increase with respect to 1976), most of them with $M_w > 5.2$ (Fig. 1a). A minimum centroid depth of 10 km was used, and some depths started to be fixed based on body waves (Fig. 1b). Depths in the 10–35 km range were rounded to the nearest kilometer. Early improvements of the routine analysis were the modeling of mantle waves (Dziewonski and Woodhouse, 1983) and consideration of lateral heterogeneities of seismic wave velocities (Woodhouse and Dziewonski, 1984, implemented at the beginning of 1984, Dziewonski *et al.*, 1984). These improvements were applied backward to seismicity from 1977 onward (e.g., Giardini *et al.*, 1985; Dziewonski *et al.*, 1987a, 1988), so I will consider the period 1977–1985 as a single one, compiled with a sufficiently homogeneous methodology.

1986–2003

During this era, the minimum centroid depth was fixed instead to 15 km (Fig. 1b), as shallower solutions were deemed unstable (Dziewonski *et al.*, 1987b). Additional methodological changes were the use of a new model of mantle shear-wave velocities (Dziewonski and Woodward, 1992) for earthquakes that occurred since July 1991 (Dziewonski *et al.*, 1992), and an improved calculation of the amplitude decay due to attenuation for those occurred since the beginning of 1994 (Dziewonski *et al.*, 1994), using a model later published by Durek and Ekström (1996). During this period, an average of 862 earthquakes per year was reported, a notable increase due to including more small earthquakes than before, as clearly noticeable for $M_w \leq 5.2$ (Fig. 1a).

2004–present

The broadband Global Seismographic Network achieved global coverage by 2004 (Butler *et al.*, 2004; Ammon *et al.*, 2010). Broadband deployments have drastically enhanced the ability to characterize smaller earthquakes and reduce M_c in the catalogs (e.g., Hutton *et al.*, 2010; González, 2017). So a similar effect is to be expected in the Global CMT.

Moreover, the CMT inversion routine, under the new lead of Göran Ekström (Ekström *et al.*, 2012), incorporated several changes and improvements at the beginning of 2004. Namely, data of intermediate-period surface waves started to be used (following the method by Arvidsson and Ekström, 1998, which allowed analyzing earthquakes smaller than before, and better determining the moment tensors of shallow ones), and modeling of the moment-rate function was improved (Ekström and Nettles, 2015). The minimum centroid depth was again changed, set as 12 km (Ekström and Nettles, 2015), and the pattern of manually fixed depths was significantly modified (Fig. 1b), for example, the value of 15 km was maintained, but the value of 33 km was almost no longer used. The latter change was actually due to a modification in the reporting of hypocentral depths in the U.S. Geological Survey National Earthquake Information Center (NEIC) catalog (noted by

Ekström, personal comm., 2024). Frequently, when a centroid depth could not be resolved, it was fixed to the hypocentral depth reported by NEIC. This institution, in turn, stopped using 33 km as a default value for fixed depths at the end of 2003. During this last period considered of the Global CMT catalog, it was achieved that the proportion of depths calculated as free parameters (73%) was significantly larger than in 1976–2003 (53%).

The magnitude and depth pattern of earthquakes in the catalog changed in 2006 simultaneously to the move of the project to a different institution. Namely, in summer 2006, the project (according to its webpage), moved with Ekström to the Lamont–Doherty Earth Observatory of Columbia University, changing its name to current one of the Global CMT Project, and being coled by Meredith Nettles. Agnew (2015) had noticed that, for 2004, 2005, and the beginning of 2006, the catalog contains more small earthquakes ($M_w < 5.0$) than immediately after. This author furthermore pointed out that, during those years, it seemed as if M_w (so indirectly the reported M_0) had been calculated differently from the rest of the catalog (Agnew, 2015, his fig. 8b). It turns out that, during those years, the new methods for analysis had been implemented, but it was still common to fix centroid depths based on the body waves, a procedure that was discontinued for the earthquakes that occurred since April 2006 onward (Fig. 1b). This change in the pattern of fixed depths has not been explicitly noticed elsewhere. Because it typically takes a few months to calculate and publish the final Global CMT solutions, the analysis of that month was finished once the project had moved to Columbia, and indeed the monthly data file in the webpage (see Data and Resources) dates from September 2006. Ekström *et al.* (2012) indicated that, since 2006, not only of earthquake locations from NEIC were used as an input for the CMT inversion, but also of locations obtained from analyzing intermediate-period surface waves (using the procedure of Ekström, 2006). This procedural change in 2006 (presumably from earthquakes of April onward) apparently resulted in not needing to fix centroid depths based on the body waves as was common before. According to Ekström (personal comm., 2024), broadband modeling of body waves was discontinued in 2006 because it was time consuming and the surface waves were found to provide better depth resolution for all earthquakes.

That M_0 values in 2004–early 2006 seem biased toward small values (Agnew, 2015) may be explained if some centroid depths had been biased toward too shallow values with the procedures used in that particular period, before that change and when fixing depths based on body waves had not been deprecated yet. This effect would arise from a possible trade-off between depth and M_0 when modeling the observed waveform amplitudes: The shallower a centroid is assumed to be, in general, the lower the calculated M_0 may be expected to be, to avoid the modeled amplitudes being too large. So both kinds of heterogeneities (on magnitudes and depths), being coincident in January 2004–March 2006, might be due to the same cause. In any case, a more detailed analysis would be required to further clarify this issue.

Despite these heterogeneities, I will consider the period 2004–2023 as a single one, given that the same minimum centroid depth was used (Fig. 1b) and, especially, since the most important improvements in monitoring and data analysis started already in 2004. Since this year, smaller and more numerous earthquakes were included in the catalog (Ekström, 2015). An average of 2201 earthquakes per year were reported between 2004 and 2023, an increase of over 250% compared to the previous period, mostly due to earthquakes with $M_w \leq 5.2$ (Fig. 1a).

Spatial and Temporal Variations of the Magnitude of Completeness (M_c)

To be meaningful, M_c has to be calculated for separated space–time volumes, since it typically increases with the distance to the seismological stations and is subject to temporal changes coincident with modifications in the methodology for compiling the catalog, and with developments of the seismological network (e.g., Hutton *et al.*, 2010; González, 2017). Only earthquakes with centroid depth ≤70 km were used (as, e.g., by Woessner and Wiemer, 2005), given that this range includes most events (82% of the total for 1977–2023) and is the most relevant for seismic hazard. It is meaningful to avoid mixing them with deeper earthquakes in the analysis, since M_c is expected to vary with depth (e.g., Kagan, 2003; Schorlemmer *et al.*, 2010).

M_c was calculated as the minimum value at which an exponential distribution of magnitudes (Gutenberg and Richter, 1944) holds, as determined by the entire-magnitude-range (EMR) method. This procedure was already applied by Woessner and Wiemer (2005) to the Global CMT catalog when proposing it. It relies on the catalog data itself and, using bootstrap resampling, provides a reliable maximum-likelihood estimate of M_c even with small samples (≥60 earthquakes) and of its standard deviation, δM_c (Woessner and Wiemer, 2005). All earthquakes with magnitude $\geq M_c$ are assumed to be detected. Below M_c, the earthquake frequencies are fitted to a cumulative normal (Gaussian) distribution, which describes how the probability of detection is reduced as the magnitude decreases. Visual inspection of the magnitude–frequency relation (e.g., Ekström *et al.*, 2012; Ekström and Nettles, 2015) typically underestimates M_c because it is not usually possible to reliably determine by eye the departure from the Gutenberg–Richter relationship (e.g., Felzer, 2008). The classical goodness-of-fit test for an exponential distribution (Lilliefors, 1969) may be suited for calculating M_c with large samples (Herrmann and Marzocchi, 2021) but has too low statistical power for small ones (e.g., Marzocchi *et al.*, 2020); indeed, tests indicated that it systematically underestimated M_c compared to EMR with the small subcatalogs here forth used. Because the Global CMT catalog does not report which seismological stations

recorded each earthquake, methods for calculating M_c based on the station distance (e.g., Schorlemmer and Woessner, 2008) cannot be properly applied.

The EMR software code (see, e.g., Mignan and Woessner, 2012) searches by default in a range of ±0.4 magnitude units around the mode of the magnitude distribution (M_c determined by maximum curvature, Wiemer and Wyss, 2000). A wider range of ±0.6 magnitude units was here used instead to avoid any potential biases.

For avoiding empty bins and providing stable results, magnitudes were binned to $\Delta M_w = 0.1$ magnitude units, which is on the order of the actual magnitude uncertainty in the catalog and the default binning for the EMR method (e.g., Mignan and Woessner, 2012). The catalog provides M_0 with 3 or 4 significant digits, allowing (taking into account the nonlinear relation to M_w) a finer nominal magnitude precision of $\Delta M_w \sim 10^{-3}$ (e.g., Navas-Portella *et al.*, 2019). But the actual magnitude uncertainties are larger. Ekström and Nettles (2015) indicated that the usual standard deviation of M_0 determinations in the catalog was <20%, which corresponds to ~0.05 units of M_w. And, when taking M_w values from the Global CMT catalog for the ISC-GEM catalog (Di Giacomo *et al.*, 2015), an uncertainty of ±0.1 magnitude units was assigned (Lee and Engdahl, 2015).

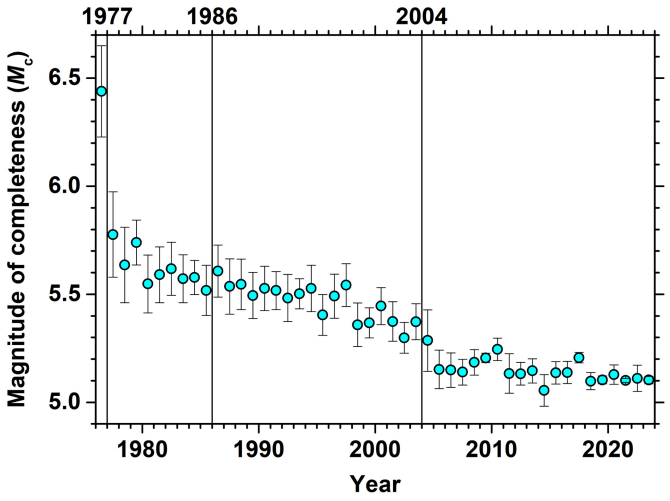

Figure 2. Mean magnitude of completeness M_c per year, for earthquakes with centroid depth ≤70 km. Error bars are ±1 δM_c, calculated from 1000 bootstraps. Dots are placed at the middle of each calendar year, and their width covers the corresponding yearly interval. Vertical lines divide periods in the catalog development, as in Figure 1. Numerical results are provided in Data S1. The color version of this figure is available only in the electronic edition.

Yearly variations of M_c

Figure 2 shows the mean M_c and the bootstrap estimate of its standard deviation, δM_c, for shallow earthquakes (centroid depth ≤70 km) per each calendar year (also presented in the Data S1). In comparison, Kagan (2003) calculated M_c in wider (5-year) periods, albeit he considered shallow, intermediate, and deep earthquakes separately. These M_c values average out the spatial variations, but provide a general overview of the catalog improvement over time. A decreasing trend is evident (Fig. 2), especially between periods, with M_c being relatively more stable within each period: ~6.4 in 1976, 5.5–5.8 in 1977–1985, 5.3–5.6 in 1986–2003, and 5.1–5.3 in 2004–2023. The stated goal of $M_c = 5.0$ (Ekström and Nettles, 2015) has not been reached yet, albeit a stable $M_c = 5.1$ has been achieved systematically, on average, since 2018.

Spatial variations of M_c in each period

Figure 3 and Videos S3–S5 show the spatial variations of M_c for each period since 1977. Such a mapping cannot be properly done in a yearly basis, as there would be too few earthquakes for analysis (e.g., for 1976). As Woessner and Wiemer (2005) did, I calculated M_c at each node of a latitude–longitude lattice, considering the earthquakes within a radius of 1000 km around it (if and only if there were at least 60 earthquakes in this spherical cap). But I used a grid spacing of 1°, instead of the 2° they employed, so the density of nodes (and map detail) is four times as large as theirs. Blank areas in the maps had too few earthquakes for calculating M_c.

Values of M_c and δM_c for each location and period, calculated using 200 bootstraps per sample, are provided as Data S2. Maps of δM_c are provided as Figure S1 and show a decreasing trend with time, being the mean values 0.15, 0.11, and 0.07, from the first to third map, respectively. This improvement results from the typically larger number of earthquakes available for analysis at each node of the map for more recent periods. Given the relatively low values of δM_c, the variability observed for M_c, both in time and space, is to a large extent systematic and statistically significant.

Overall, along 1977–2023, M_c varied between 5.0 and 6.0, depending on the period and location. In 1977–1985, $M_c \in [5.5,6.0]$, with an irregular spatial pattern. In 1986–2003, $M_c \in [5.3,6.0]$, being the highest (worst) values found between Tasmania and Antarctica, but with a general improvement in other regions, compared with the former period. For 2004–2023 the map is particularly detailed, thanks to the abundance of data; $M_c \in [5.0,5.5]$, a significant reduction compared to the previous era, with low values in well monitored regions (e.g., Japan, Taiwan, western Mediterranean, and west coast of North America, see, e.g., maps of contributing stations in 2010 and 2012 (Ekström *et al.*, 2012; Ekström and Nettles, 2015, respectively). The highest M_c values since 2004 are again found in remote offshore areas near Antarctica, far away from any station.

In this last period, even considering the uncertainties and rounding of the digits, the goal of $M_c = 5.0$ (Ekström and Nettles, 2015) was reached only in a minority of regions.

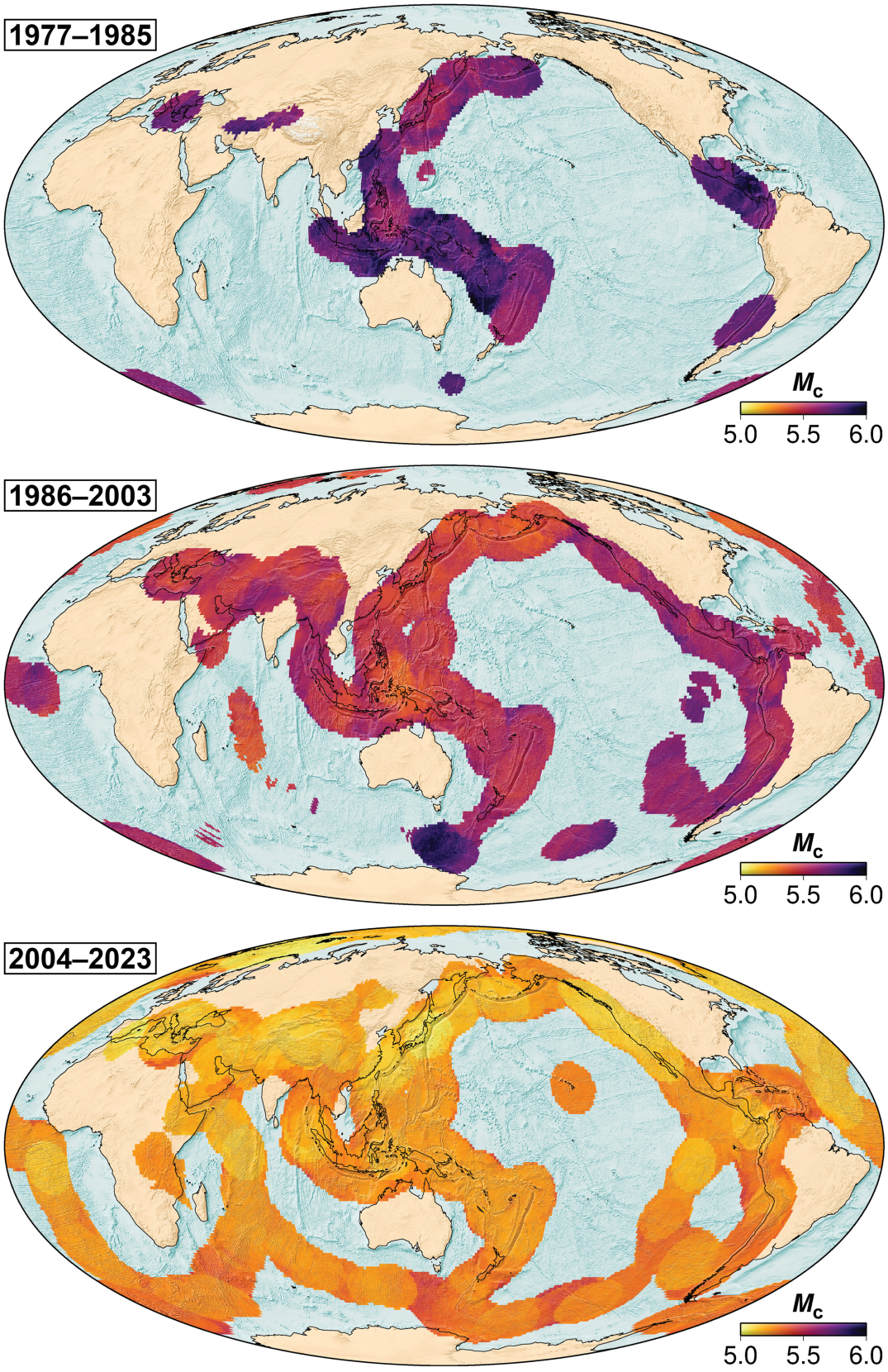

Figure 3. Magnitude of completeness (M_c) in the periods indicated. The Mollweide (equal area) projection is centered on longitude 150° E to better show the land areas around the circum-Pacific rim. Note the identical color scale for the three maps. Numerical results are provided in Data S2. Animated, rotating versions of these globes are presented in Videos S3–S5.

Namely, it is statistically higher, beyond two standard deviations ($M_c - 2\delta M_c > 5.05$) in 57% of the map area where it could be determined (weighting the latitude–longitude points of the map by the area of the cells they represent, see González, 2010), and in particular, in most of the southern hemisphere.

Indeed, since 1986, when spatial trends are most apparent, the lowest M_c values are systematically found in the northern hemisphere, and the highest ones in the southern hemisphere (Fig. 3). This asymmetry was also noted, with less detail, by Johnston and Halchuk (1993) and Woessner and Wiemer (2005), and is expected from the majority of seismological stations being located in the northern hemisphere, allowing a better coverage (both because of the spatial density of stations and the network geometry). Gaebler and Ceranna (2021) calculated a similar hemispherical asymmetry for the detectability of the International Monitoring System Seismic Network. Ringler *et al.* (2024) also calculated a similar pattern for the global m_b detection thresholds of the network used by NEIC.

In addition, systematic spatial differences in M_c may be due to an unintentional selection bias (initially suggested by Ekström, personal comm., 2021) caused by regionally variable discrepancies between M_w and body-wave magnitude m_b. Since 2004, the selection criteria for attempting a CMT analysis (Ekström *et al.*, 2012; Ekström and Nettles, 2015) is that the earthquake has a reported magnitude (m_b or surface-wave magnitude M_s) ≥4.8, usually considering the preliminary determination of hypocenters (PDE) catalog of NEIC. Acknowledging the differences between magnitude scales, and the uncertainties in magnitude determination, this threshold aims to include all earthquakes with $M_w \geq 5.0$ (Ekström and Nettles, 2015). For most earthquakes around that threshold (especially those recorded at teleseismic distances), the magnitude type reported by PDE is m_b. These m_b values are, on average, similar to the final, reviewed ones determined by ISC (e.g., Rezapour and Pearce, 1998; Scordilis, 2006). M_w and m_b scale differently with M_0, so the difference $M_w - m_b$ is not constant. Moreover, there are systematic regional variations in the average difference between the final m_b values from ISC and M_w (Lolli *et al.*, 2014, 2015): in regions of high body-wave attenuation (such as mid-ocean ridges, especially in the Pacific), m_b tends to be underestimated, whereas in regions with low attenuation (such as in continental interiors and several subduction zones, e.g., in the western Pacific) it tends to be overestimated. So the larger the average difference $M_w - m_b$ is in a region, the higher the actual M_w selection threshold of the Global CMT catalog may be (and the higher M_c would tend to be).

This inadvertent selection bias may, for example, have contributed to the high M_c in midocean ridges (which, in addition, are located far away from most seismological stations), and to the low M_c in subduction zones in the western Pacific, and in central Asia. For the latter, Patton (1998) and Patton and Randall (2002) found that M_0 values from the Global CMT may be typically overestimated by a factor of ∼2, so M_w and thus M_c would tend to be too high by ∼0.2 units of M_w on average. But there the mean observed difference $M_w - m_b$ is on the order of −0.3 to −0.4 (Lolli *et al.*, 2014, their fig. 2), contributing to reduce M_c much further, consistently with the low values observed. So this selection bias may even counteract others. Conversely, since 2006 the catalog compilers also calculate an independent magnitude estimate based on intermediate-period surface waves to check whether a CMT inversion could be attempted (Ekström *et al.*, 2012), a procedure which may compensate the effect of this selection bias, to an unknown extent, which would merit further scrutiny.

Interestingly, since 2004 the lowest M_c is observed in the northern mid-Atlantic Ridge (Arctic Ocean). There, m_b is underestimated with respect to M_w (compare M_w and the classical m_b based on *P* waves in table 1 of Kim *et al.*, 2020). So, instead, a high M_c would be expected from the threshold selection bias. The low M_c may be due to the relatively dense monitoring of this area: for example, the map of contributing stations to the catalog in 2012 (Ekström and Nettles, 2015) shows a dense network around it, with good azimuthal coverage, being similar the number of stations in Greenland to those on western Europe.

In northern Sumatra and surroundings, M_c is intriguingly low in the last period (Fig. 3). There the network of contributing stations is not dense (maps by Ekström *et al.*, 2012 and Ekström and Nettles, 2015 show no station in Sumatra), and M_c was not low in 1986–2003 (Fig. 3). This reduction of M_c might be due to several reasons. First, the general improvement of the global monitoring network. Second, given that the prolific aftershock sequence of the great 2004 earthquake was studied in detail by the catalog compilers (Lay *et al.*, 2005), there could be some lowering of M_c due to this focused analysis. And third, this aftershock sequence involved an extraordinarily energetic swarm (Lay *et al.*, 2005), implying a change in the regional magnitude distribution which might have affected the estimation of M_c.

As a cautionary note, the M_c values calculated here are, inevitably, averages for each location and period considered. Yearly values for global seismicity (Fig. 2) are barely sensitive to spatial variations. And maps for each period (Fig. 3) may not be representative of temporal variations at smaller time scales. In addition, M_c may increase during seismic sequences (e.g., Hainzl, 2016) because of the overlap of the seismograms of earthquakes occurring shortly after each other, which hampers event detection and analysis (e.g., Jia *et al.*, 2022). This effect implies that large earthquakes can be missing in the coda of even larger ones (Ekström and Nettles, 2015); it has been quantified in the Global CMT catalog for aftershock sequences (Kagan, 2003, 2004) and for worldwide seismicity (Iwata, 2008, 2012).

Spatial Depth Heterogeneities

Because shallow earthquakes are more frequently assigned a fixed depth in the catalog, previously unnoticed regional

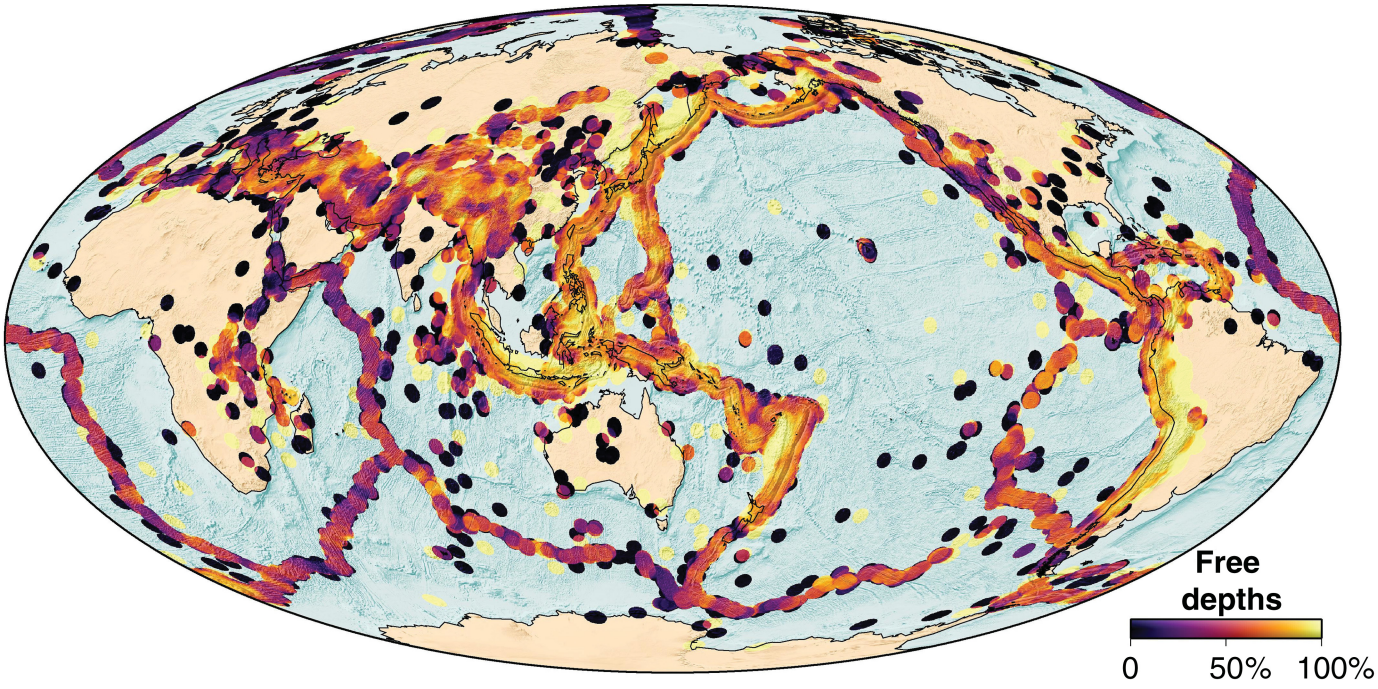

Figure 4. Percentage of centroid depths calculated as free parameters (i.e., not fixed), during 1976–2023, using a spatial moving average with 200 km radius.

variations of depth quality can be identified (Fig. 4). High quality, free, depth determinations are systematically more common in the deep parts of subduction zones (e.g., South America, Tonga, Indonesia, and Kamtchatka–Kuriles) and are less so in midocean ridges, the shallow part of subduction zones, and other regions with shallow seismicity (e.g., California).

Temporal Rake Heterogeneities

The catalog reports the two possible rake angle values for each earthquake (in the range [−180,180]) using the convention of Aki and Richards (2009): −180°, 0° or +180° for pure strike slip, −90° for pure normal slip, and +90° for pure reverse slip.

The online format description of the catalog (see Data and Resources) notes that, for some shallow earthquakes, the vertical dip-slip components of the moment tensor could not be determined properly in the CMT inversion, and they were fixed as zero. In those cases, the result is that the mechanism is assumed as pure (so the rake is exactly either −180°, −90°, 0°, +90°, or +180°). It is not averted, though, that this procedure was used almost exclusively before 2004: for 686 earthquakes between 1976 and 2003, but only for two afterward.

Figure 5 shows the rake histograms (considering both rake values per each earthquake), separated in those two broad periods. There is an overall, periodic variation in the frequency of the rake angle, with values close to pure mechanisms being more frequent than intermediate ones (Petruccelli *et al.*, 2018).

However, the pattern is different in these two periods. Before 2004 there are spikes of excess frequency of pure mechanisms (due to zeroing of vertical dip-slip components for some earthquakes). In addition, since 2004, the peaks around pure mechanisms tend to be narrower than in the earlier times. Moreover, the peak at 0° for 1976–2003, with the spike removed, would be lower than those for −180°, −90°, and 180°, whereas in 2004 those four peaks have similar height. So the histograms in both periods would not become equivalent just by disregarding the spikes.

It has to be concluded that the reported rakes and focal mechanisms have been systematically different before and after the methodological improvements introduced in 2004. These heterogeneities were not noticed in earlier analyses, for example by Petruccelli *et al.* (2018), who binned more coarsely the rake angles in their histograms, nor by Taroni and Selva (2021), who used focal mechanisms for earthquakes that occurred since 2004 to retrospectively forecast earlier mechanisms.

Temporal Heterogeneities of the Double-Couple Component

The double-couple component C_{DC} can be calculated from the moment tensor eigenvalues and scalar seismic moment reported in the catalog (e.g., Vavryčuk, 2015). Zaccagnino and Doglioni (2022) showed that it varies as a function of rake in the Global CMT catalog and the ISC Bulletin, and interpreted this dependence in physical terms. Alternatively, it has been commonly proposed that non-double-couple components are artifacts of moment tensor inversion (e.g., Wimpenny and Watson, 2021; Rösler *et al.*, 2024).

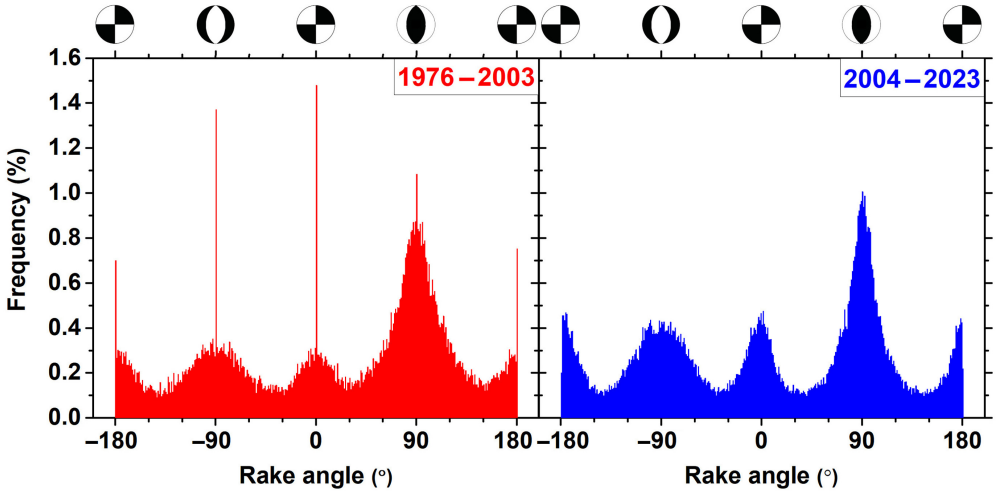

Figure 5. Histograms of the rake angles in two broad periods (years 1976–2003 and 2004–2023), separated by a major change in methods for centroid determination. Spikes in the first period are due to earthquakes for which vertical dip-slip components of the moment tensor could not be resolved and were set as zero. The focal sphere projections plotted on top illustrate, for reference, pure mechanisms at their respective rake angles. The color version of this figure is available only in the electronic edition.

Trying to shed light on this controversy, here I explore whether there are temporal heterogeneities of C_{DC} in the Global CMT catalog as a function of the reported rake. Figure 6 shows the results for all earthquakes, regardless of depth or magnitude, and considering both rakes reported for each earthquake. Qualitatively similar results are obtained if only shallow earthquakes are considered (≤50 km as Zaccagnino and Doglioni, 2022). Indeed, differences are unveiled when the catalog is split into two broad periods (1976–2003 and 2004–2023). In the most recent one, C_{DC} depends more markedly on the rake angle. For example, thrust events (rake about +90°) or normal ones (rake about −90°) have a significantly higher mean C_{DC} in 2004–2023 than in 1976–2003. And a lower C_{DC} is observed for transtensional earthquakes (rake intermediate between −90° and −180° or −90° and 0°). These variations cannot be explained by the lower magnitudes recorded in the second period, because larger earthquakes tend to have higher C_{DC} (Rösler *et al.*, 2021), at least those with thrust or transpressional mechanisms (Zaccagnino and Doglioni, 2022), whereas the larger C_{DC} is observed for such mechanisms in the second period, which has many more earthquakes of relatively low magnitudes. So, again, these temporal differences in the C_{DC} are most likely due to the systematic differences in focal mechanism determinations between these two broad periods in the catalog.

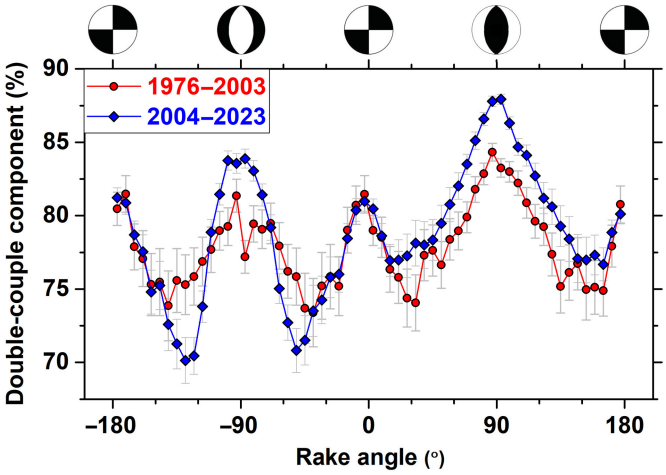

Figure 6. Variation of the double-couple component as a function of rake angle, for two broad periods of the catalog (years labeled). Dots are the mean value, calculated using bins of 6° for the rake angle. Error bars are twice the standard deviation of the mean (bias-corrected sample standard deviation divided by the square root of the number of values in each bin). The color version of this figure is available only in the electronic edition.

The systematic variation of C_{DC} with the rake angle seems inconsistent with an exclusive origin as an artifact of the moment tensor inversion and points toward a partial physical origin (compare with Zaccagnino and Doglioni, 2022). Indeed, such variations are more evident in the recent period of the catalog, when the mechanisms were calculated with an improved methodology and are expected to be the most reliable. But the differences observed between the two periods analyzed, during which different inversion methods were used, points out that indeed part of the variation is an artifact due to the inversion (compare with Rösler *et al.*, 2024).

Conclusions

Albeit it is usually claimed that the Global CMT catalog is "uniform in its methodology" (Ekström and Nettles, 2015), the latter has experienced a number of improvements, resulting in catalog heterogeneities that so far had not been characterized in detail or had been directly unnoticed.

As with other catalog analyses, this work started by considering eras in the catalog development, and their imprint on the catalog (for example, in the rate of earthquakes included per year, the minimum depth used, and the way some depths were fixed). I correlate the magnitude heterogeneities first noticed by Agnew (2015) for 2004, 2005,

and early 2006 with the procedures then used for calculating centroid depths.

The magnitude of completeness (M_c) of the catalog is determined here with an objective method, in unprecedented detail. It shows a general improvement toward lower values over time, correlated with the methodological improvements. And it has significant heterogeneities in space, which can be explained by the proximity to seismological stations, by unintentional selection biases due to regional differences between body-wave magnitudes and moment magnitudes, and, exceptionally, by possible, deliberate selection biases. The goal of $M_c = 5.0$ (Ekström and Nettles, 2015) has been reached only in some regions of the northern hemisphere since 2004, but not globally.

Regional differences in the quality of the depth determinations are found, due to the preferential fixing of the depths of shallow earthquakes, which are more frequent in some regions than in others.

Both the frequency distribution of rakes and the distribution of the double-couple component as a function of the on the rake angle indicate that moment tensor determinations in 1976–2003 cannot be considered equivalent to those in 2004–2023. In the last period, when such determinations are more reliable, the variations in such distributions are clearer.

The heterogeneities shown here should be considered when analyzing the catalog or using it as a source for other databases. These results could be particularly valuable when developing and testing earthquake forecast models, procedures that require a complete catalog. Assuming a too low M_c may bias the results, whereas the opposite reduces unnecessarily the available number of earthquakes for analysis (e.g., Mizrahi *et al.*, 2021). For example, Kagan and Jackson (2011) considered only earthquakes with $M_w \geq 5.8$, as they deemed the catalog incomplete for smaller ones. But since 2004, it is shown here that $M_c \leq 5.5$, even considering temporal and spatial heterogeneities. Lowering the magnitude threshold of analysis allows building more detailed and robust models, and testing them with more events in a shorter time span, instead of waiting for years or decades until enough target earthquakes, not used for the model development, take place (e.g., Eberhard *et al.*, 2012; Taroni *et al.*, 2014).

Finally, models in which focal mechanisms of a given period are used to forecast those of a different period (e.g., Kagan and Jackson, 2014; Taroni and Selva, 2021) will be affected by the temporal heterogeneity of the focal mechanism determinations identified in this work, so further insights on the impact of these heterogeneities would be required.

Data and Resources

The data were obtained from the Global Centroid Moment Tensor (Global CMT) project, from the files available at www.globalcmt.org/CMTfiles.html. Maps were plotted using Generic Mapping Tools (GMT) (Wessel *et al.*, 2019; Wessel, 2024), using perceptually uniform color palettes: *lajolla* (Fig. 4; Crameri, 2018 and Crameri *et al.*, 2020); *inferno* (Fig. 3 and Videos S3–S5) and *viridis* (Fig. S1) by Stefan van der Walt and Nathaniel Smith (https://bids.github.io/colormap). All websites were last accessed in April 2024. The supplemental material includes: Figure S1: maps of δM_c. Video S1: A rotating blank Earth (for reference); Video S2: Rotating map of epicentroids of the Global CMT catalog (1976–2023) plotted in order of increasing magnitude; Videos S3–S5: rotating M_c maps for the three periods considered, as labeled. Data S1: values of M_c and δM_c per year (as in Fig. 2). Data S2: values of M_c shown in Figure 2 and Videos S3–S5, and of δM_c shown in Figure S1.

Declaration of Competing Interests

The author acknowledges that there are no conflicts of interest recorded.

Acknowledgments

Thanks are due to the Global Centroid Moment Tensor (Global CMT) project for the invaluable data provided over the decades. Göran Ekström and an anonymous reviewer provided wise and encouraging comments on the initial article. Valuable discussions with Marcus Hermann and Warner Marzocchi on the estimation of M_c are also appreciated. This research initially benefited from economic support by the GeoForschungsZentrum (GFZ) German Research Centre for Geosciences and the European Union's Horizon 2020 research and innovation program (Grant Number 821115, Real-Time Earthquake Risk Reduction for a Resilient Europe [RISE]). It was finalized thanks to two grants of the Spanish Research Agency (agency code MCIN/AEI/ 10.13039/501100011033): IJC2020-043372-I (supported by the European Union Next Generation EU/PRTR) and PID2021-125979OB-I00 (supported by the European Union ERDF). The author would like to devote this article as a tribute to Yan Y. Kagan and David D. Jackson, with whom he was fortunate to exchange stimulating discussions on earthquake catalogs and testing of earthquake forecasts, and to Pål Wessel, for unselfishly leading the Generic Mapping Tools (GMT) project for the whole Earth Sciences community.

References

Agnew, D. C. (2015). Equalized plot scales for exploring seismicity data, *Seismol. Res. Lett.* **86,** no. 5, 1412–1423, doi: 10.1785/0220150054.

Aki, K., and P. G. Richards (2009). *Quantitative Seismology*, Second Ed., University Science Books, Sausalito, California, 700 pp.

Ammon, C. J., T. Lay, and D. W. Simpson (2010). Great earthquakes and global seismic networks, *Seismol. Res. Lett.* **81,** no. 6, 965–971, doi: 10.1785/gssrl.81.6.965.

Arvidsson, R., and G. Ekström (1998). Global CMT analysis of moderate earthquakes, $M_w \geq 4.5$, using intermediate-period surface waves, *Bull. Seismol. Soc. Am.* **88,** no. 4, 1003–1013, doi: 10.1785/BSSA0880041003.

Bird, P., D. D. Jackson, Y. Y. Kagan, C. Kreemer, and R. S. Stein (2015). GEAR1: A global earthquake activity rate model constructed from geodetic strain rates and smoothed seismicity, *Bull. Seismol. Soc. Am.* **105,** no. 5, 2538–2554, doi: 10.1785/0120150058.

Bormann, P. (2015). Are new data suggesting a revision of the current M_w and M_e scaling formulas? *J. Seismol.* **19,** no. 4, 989–1002, doi: 10.1007/s10950-015-9507-y.

Butler, R., T. Lay, K. Creager, P. Earl, K. Fischer, J. Gaherty, G. Laske, B. Leith, J. Park, M. Ritzwolle, *et al.* (2004). The Global Seismographic Network surpasses its design goal, *Eos Trans. AGU* **85,** no. 23, 225–229, doi: 10.1029/2004EO230001.

Corral, Á., and Á. González (2019). Power law size distributions in geoscience revisited, *Earth Space Sci.* **6,** 673–697, doi: 10.1029/2018EA000479.

Crameri, F. (2018). Geodynamic diagnostics, scientific visualisation and StagLab 3.0, *Geosci. Model Dev.* **11,** no. 6, 2541–2562, doi: 10.5194/gmd-11-2541-2018.

Crameri, F., G. E. Shephard, and P. J. Heron (2020). The misuse of colour in science communication, *Nat. Commun.* **11,** no. 1, 5444, doi: 10.1038/s41467-020-19160-7.

Deichmann, N. (2018). The relation between M_E, M_L and M_w in theory and numerical simulations for small to moderate earthquakes, *J. Seismol.* **22,** no. 6, 1645–1668, doi: 10.1007/s10950-018-9786-1.

Di Giacomo, D., and D. A. Storchak (2016). A scheme to set preferred magnitudes in the ISC bulletin, *J. Seismol.* **20,** no. 2, 555–567, doi: 10.1007/s10950-015-9543-7.

Di Giacomo, D., I. Bondár, D. A. Storchak, E. R. Engdahl, P. Bormann, and J. Harris (2015). ISC-GEM: Global Instrumental Earthquake Catalogue (1900–2009), III. Re-computed M_s and m_b, proxy M_w, final magnitude composition and completeness assessment, *Phys. Earth Planet. Inter.* **239,** 33–47, doi: 10.1016/j.pepi.2014.06.005.

Di Giacomo, D., E. R. Engdahl, and D. A. Storchak (2018). The ISC-GEM Earthquake Catalogue (1904–2014): Status after the extension project, *Earth Syst. Sci. Data* **10,** 1877–1899, doi: 10.5194/essd-10-1877-2018.

Di Giacomo, D., J. Harris, and D. A. Storchak (2021). Complementing regional moment magnitudes to GCMT: A perspective from the rebuilt International Seismological Centre Bulletin, *Earth Syst. Sci. Data* **13,** no. 5, 1957–1985, doi: 10.5194/essd-13-1957-2021.

Durek, J. J., and G. Ekström (1996). A radial model of anelasticity consistent with long-period surface-wave attenuation, *Bull. Seismol. Soc. Am.* **86,** no. 1A, 144–158, doi: 10.1785/BSSA08601A0144.

Dziewonski, A. M., and J. H. Woodhouse (1983). An experiment in systematic study of global seismicity: Centroid-moment tensor solutions for 201 moderate and large earthquakes of 1981, *J. Geophys. Res.* **88,** no. B4, 3247–3271, doi: 10.1029/JB088iB04p03247.

Dziewonski, A. M., and R. L. Woodward (1992). Acoustic imaging at the planetary scale, in *Acoustical Imaging*, H. Ermert and H.-P. Harjes (Editors), Vol. 19, Springer US, Boston, Massachusetts, 785–797, doi: 10.1007/978-1-4615-3370-2_124.

Dziewonski, A. M., T.-A. Chou, and J. H. Woodhouse (1981). Determination of earthquake source parameters from waveform data for studies of global and regional seismicity, *J. Geophys. Res.* **86,** no. B4, 2825–2852, doi: 10.1029/JB086iB04p02825.

Dziewonski, A. M., G. Ekström, J. E. Franzen, and J. H. Woodhouse (1987a). Global seismicity of 1977: Centroid-moment tensor solutions for 471 earthquakes, *Phys. Earth Planet. Inter.* **45,** no. 1, 11–36, doi: 10.1016/0031-9201(87)90194-4.

Dziewonski, A. M., G. Ekström, J. E. Franzen, and J. H. Woodhouse (1987b). Centroid-moment tensor solutions for January-March 1986, *Phys. Earth Planet. Inter.* **45,** no. 1, 1–10, doi: 10.1016/0031-9201(87)90193-2.

Dziewonski, A. M., G. Ekström, J. E. Franzen, and J. H. Woodhouse (1988). Global seismicity of 1981: Centroid-moment tensor solutions for 542 earthquakes, *Phys. Earth Planet. Inter.* **50,** no. 2, 155–182, doi: 10.1016/0031-9201(88)90004-0.

Dziewonski, A. M., G. Ekström, and M. P. Salganik (1992). Centroid-moment tensor solutions for July–September 1991, *Phys. Earth Planet. Inter.* **72,** no. 1–2, 1–11, doi: 10.1016/0031-9201(92)90044-V.

Dziewonski, A. M., G. Ekström, and M. P. Salganik (1994). Centroid-moment tensor solutions for January–March 1994, *Phys. Earth Planet. Inter.* **86,** no. 4, 253–261, doi: 10.1016/0031-9201(94)90124-4.

Dziewonski, A. M., J. E. Franzen, and J. H. Woodhouse (1984). Centroid-moment tensor solutions for January–March, 1984, *Phys. Earth Planet. Inter.* **34,** no. 4, 209–219, doi: 10.1016/0031-9201(84)90062-1.

Eberhard, D. A. J., J. D. Zechar, and S. Wiemer (2012). A prospective earthquake forecast experiment in the western Pacific, *Geophys. J. Int.* **190,** no. 3, 1579–1592, doi: 10.1111/j.1365-246X.2012.05548.x.

Ekström, G. (2006). Global detection and location of seismic sources by using surface waves, *Bull. Seismol. Soc. Am.* **96,** no. 4A, 1201–1212, doi: 10.1785/0120050175.

Ekström, G. (2015). Global seismicity: Results from systematic waveform analyses, 1976–2012, in *Treatise on Geophysics*, G. Schubert (Editor), 2nd ed., Vol. 4, Elsevier, 467–475, doi: 10.1016/B978-0-444-53802-4.00085-3.

Ekström, G., and M. Nettles (1997). Calibration of the HGLP seismograph network and centroid-moment tensor analysis of significant earthquakes of 1976, *Phys. Earth Planet. Inter.* **101,** nos. 3/4, 219–243, doi: 10.1016/S0031-9201(97)00002-2.

Ekström, G., and M. Nettles (2015). Long-period moment-tensor inversion: The Global CMT project, in *Encyclopedia of Earthquake Engineering*, M. Beer, I. A. Kougioumtzoglou, E. Patelli, and S.-K. Au (Editors), Springer-Verlag, Berlin and Heidelberg, 1360–1371, doi: 10.1007/978-3-642-35344-4_291.

Ekström, G., M. Nettles, and A. M. Dziewoński (2012). The Global CMT project 2004–2010: Centroid-moment tensors for 13,017 earthquakes, *Phys. Earth Planet. Inter.* **200–201,** 1–9, doi: 10.1016/j.pepi.2012.04.002.

Felzer, K. R. (2008). Calculating California seismicity rates. Appendix I in: The Uniform California Earthquake Rupture Forecast, version 2 (UCERF 2), *U.S. Geol. Surv. Open-File Rept. 2007-1437I and California Geol. Surv. Special Rept. 203I*, 127 pp., available at http://pubs.usgs.gov/of/2007/1437/i/ (last accessed June 2024).

Ferreira, A. M. G., and J. H. Woodhouse (2006). Long-period seismic source inversions using global tomographic models, *Geophys. J. Int.* **166,** no. 3, 1178–1192, doi: 10.1111/j.1365-246X.2006.03003.x.

Gaebler, P. J., and L. Ceranna (2021). Performance of the International Monitoring System Seismic Network based on ambient seismic noise measurements, *Pure Appl. Geophys.* **178,** no. 7, 2419–2436, doi: 10.1007/s00024-020-02604-y.

Giardini, D., A. M. Dziewonski, and J. H. Woodhouse (1985). Centroid-moment tensor solutions for 113 large earthquakes in 1977–1980, *Phys. Earth Planet. Inter.* **40,** no. 4, 259–272, doi: 10.1016/0031-9201(85)90037-8.

González, Á. (2010). Measurement of areas on a sphere using Fibonacci and latitude–longitude lattices, *Math. Geosci.* **42,** no. 1, 49–64, doi: 10.1007/s11004-009-9257-x.

González, Á. (2017). The Spanish National Earthquake Catalogue: Evolution, precision and completeness, *J. Seismol.* **21,** no. 3, 435–471, doi: 10.1007/s10950-016-9610-8.

Gutenberg, B., and C. F. Richter (1944). Frequency of earthquakes in California, *Bull. Seismol. Soc. Am.* **34,** no. 4, 185–188, doi: 10.1785/BSSA0340040185.

Hainzl, S. (2016). Rate-dependent incompleteness of earthquake catalogs, *Seismol. Res. Lett.* **87,** no. 2A, 337–344, doi: 10.1785/0220150211.

Hanks, T. C., and H. Kanamori (1979). A moment magnitude scale, *J. Geophys. Res.* **84,** no. B5, 2348, doi: 10.1029/JB084iB05p02348.

Hejrani, B., and H. Tkalčić (2020). Resolvability of the centroid-moment-tensors for shallow seismic sources and improvements from modeling high-frequency waveforms, *J. Geophys. Res.* **125,** no. 7, e2020JB019643, doi: 10.1029/2020JB019643.

Herrmann, M., and W. Marzocchi (2021). Inconsistencies and lurking pitfalls in the magnitude–frequency distribution of high-resolution earthquake catalogs, *Seismol. Res. Lett.* **92,** no. 2A, 909–922, doi: 10.1785/0220200337.

Hjörleifsdóttir, V., and G. Ekström (2010). Effects of three-dimensional Earth structure on CMT earthquake parameters, *Phys. Earth Planet. Inter.* **179,** nos. 3/4, 178–190, doi: 10.1016/j.pepi.2009.11.003.

Hutton, K., J. Woessner, and E. Hauksson (2010). Earthquake monitoring in southern California for seventy-seven years (1932-2008), *Bull. Seismol. Soc. Am.* **100,** no. 2, 423–446, doi: 10.1785/0120090130.

International Seismological Centre (2024). On-line bulletin, doi: 10.31905/D808B830.

Iwata, T. (2008). Low detection capability of global earthquakes after the occurrence of large earthquakes: Investigation of the Harvard CMT catalogue, *Geophys. J. Int.* **174,** no. 3, 849–856, doi: 10.1111/j.1365-246X.2008.03864.x.

Iwata, T. (2012). Revisiting the global detection capability of earthquakes during the period immediately after a large earthquake: Considering the influence of intermediate-depth and deep earthquakes, *Res. Geophys.* **2,** no. 1, 24–28, doi: 10.4081/rg.2012.e4.

Jia, Z., Z. Zhan, and H. Kanamori (2022). The 2021 South Sandwich Island M_w 8.2 earthquake: A slow event sandwiched between regular ruptures, *Geophys. Res. Lett.* **49,** no. 3, e2021GL097104, doi: 10.1029/2021GL097104.

Johnston, A. C., and S. Halchuk (1993). The seismicity data base for the Global Seismic Hazard Assessment Program, *Ann. Geofis.* **36,** nos. 3/4, 133–151, doi: 10.4401/ag-4260.

Kagan, Y. Y. (2003). Accuracy of modern global earthquake catalogs, *Phys. Earth Planet. Inter.* **135,** nos. 2/3, 173–209, doi: 10.1016/S0031-9201(02)00214-5.

Kagan, Y. Y. (2004). Short-term properties of earthquake catalogs and models of earthquake source, *Bull. Seismol. Soc. Am.* **94,** no. 4, 1207–1228, doi: 10.1785/012003098.

Kagan, Y. Y., and D. D. Jackson (2011). Global earthquake forecasts, *Geophys. J. Int.* **184,** no. 2, 759–776, doi: 10.1111/j.1365-246X.2010.04857.x.

Kagan, Y. Y., and D. D. Jackson (2014). Statistical earthquake focal mechanism forecasts, *Geophys. J. Int.* **197,** no. 1, 620–629, doi: 10.1093/gji/ggu015.

Kagan, Y. Y., and D. D. Jackson (2016). Earthquake rate and magnitude distributions of great earthquakes for use in global forecasts, *Geophys. J. Int.* **206,** no. 1, 630–643, doi: 10.1093/gji/ggw161.

Kanamori, H. (1977). The energy release in great earthquakes, *J. Geophys. Res.* **82,** no. 20, 2981–2987, doi: 10.1029/JB082i020p02981.

Kim, W.-Y., L. Ottemöller, and P. G. Richards (2020). A Regional *Sn* magnitude scale $m_b(Sn)$ and estimates of moment magnitude for earthquakes along the northern Mid-Atlantic Ridge, *Bull. Seismol. Soc. Am.* **110,** no. 6, 3158–3173, doi: 10.1785/0120190304.

Lay, T., H. Kanamori, C. J. Ammon, M. Nettles, S. N. Ward, R. C. Aster, S. L. Beck, S. L. Bilek, M. R. Brudzinski, R. Butler, *et al.* (2005). The Great Sumatra-Andaman earthquake of 26 December 2004, *Science* **308,** no. 5725, 1127–1133, doi: 10.1126/science.1112250.

Lee, W. H. K., and E. R. Engdahl (2015). Bibliographical search for reliable seismic moments of large earthquakes during 1900–1979 to compute M_w in the ISC-GEM Global Instrumental Reference Earthquake Catalogue, *Phys. Earth Planet. Inter.* **239,** 25–32, doi: 10.1016/j.pepi.2014.06.004.

Lentas, K., D. Di Giacomo, J. Harris, and D. A. Storchak (2019). The ISC Bulletin as a comprehensive source of earthquake source mechanisms, *Earth Syst. Sci. Data* **11,** 565–578, doi: 10.5194/essd-11-565-2019.

Lilliefors, H. W. (1969). On the Kolmogorov–Smirnov test for the exponential distribution with mean unknown, *J. Am. Stat. Assoc.* **64,** no. 325, 387–389, doi: 10.1080/01621459.1969.10500983.

Lolli, B., P. Gasperini, and G. Vannucci (2014). Empirical conversion between teleseismic magnitudes (m_b and M_s) and moment magnitude (M_w) at the Global, Euro-Mediterranean and Italian scale, *Geophys. J. Int.* **199,** no. 2, 805–828, doi: 10.1093/gji/ggu264.

Lolli, B., P. Gasperini, and G. Vannucci (2015). Erratum: Empirical conversion between teleseismic magnitudes (m_b and M_s) and moment magnitude (M_w) at the Global, Euro-Mediterranean and Italian scale, *Geophys. J. Int.* **200,** no. 1, 199, doi: 10.1093/gji/ggu385.

Marzocchi, W., I. Spassiani, A. Stallone, and M. Taroni (2020). How to be fooled searching for significant variations of the *b*-value, *Geophys. J. Int.* **220,** no. 3, 1845–1856, doi: 10.1093/gji/ggz541.

Mignan, A., and J. Woessner (2012). Estimating the magnitude of completeness for earthquake catalogs, *Community Online Resource for Statistical Seismicity Analysis*, doi: 10.5078/CORSSA-00180805.

Mizrahi, L., S. Nandan, and S. Wiemer (2021). Embracing data incompleteness for better earthquake forecasting, *J. Geophys. Res.* **126,** no. 12, e2021JB022379, doi: 10.1029/2021JB022379.

Morales-Yáñez, C., Z. Duputel, and L. Rivera (2020). Impact of 3-D Earth structure on W-phase CMT parameters, *Geophys. J. Int.* **223,** no. 2, 1432–1445, doi: 10.1093/gji/ggaa377.

Mueller, C. S. (2019). Earthquake catalogs for the USGS national seismic hazard maps, *Seismol. Res. Lett.* **90,** no. 1, 251–261, doi: 10.1785/0220170108.

Navas-Portella, V., Á. González, I. Serra, E. Vives, and Á. Corral (2019). Universality of power-law exponents by means of maximum-likelihood estimation, *Phys. Rev. E* **100,** no. 6, 062106, doi: 10.1103/PhysRevE.100.062106.

Patton, H. J. (1998). Bias in the centroid moment tensor for central Asian earthquakes: Evidence from regional surface wave data, *J. Geophys. Res.* **103,** no. B11, 26,963–26,974, doi: 10.1029/98JB02529.

Patton, H. J., and G. E. Randall (2002). On the causes of biased estimates of seismic moment for earthquakes in central Asia, *J. Geophys. Res.* **107,** no. B11, 2302, doi: 10.1029/2001JB000351.

Petruccelli, A., D. Schorlemmer, T. Tormann, A. P. Rinaldi, S. Wiemer, P. Gasperini, and G. Vannucci (2019). The influence of faulting style

on the size-distribution of global earthquakes, *Earth Planet. Sci. Lett.* **527,** 115791, doi: 10.1016/j.epsl.2019.115791.

Petruccelli, A., G. Vannucci, B. Lolli, and P. Gasperini (2018). Harmonic fluctuation of the slope of the frequency–magnitude distribution (*b*-value) as a function of the angle of rake, *Bull. Seismol. Soc. Am.* **108,** no. 4, 1864–1876, doi: 10.1785/0120170328.

Rezapour, M., and R. G. Pearce (1998). Bias in surface-wave magnitude M_s due to inadequate distance corrections, *Bull. Seismol. Soc. Am.* **88,** no. 1, 43–61, doi: 10.1785/BSSA0880010043.

Ringler, A. T., D. C. Wilson, P. Earle, W. Yeck, D. B. Mason, and J. Wilgus (2024). Noise constraints on global body-wave measurement thresholds, *Bull. Seismol. Soc. Am.* doi: 10.1785/0120230246.

Rösler, B., S. Stein, A. Ringler, and J. Vackář (2024). Apparent non-double-couple components as artifacts of moment tensor inversion, *Seismica* **3,** no. 1, doi: 10.26443/seismica.v3i1.1157.

Rösler, B., S. Stein, and B. D. Spencer (2021). Uncertainties in seismic moment tensors inferred from differences between global catalogs, *Seismol. Res. Lett.* **92,** no. 6, 3698–3711, doi: 10.1785/0220210066.

Sawade, L., S. Beller, W. Lei, and J. Tromp (2022). Global centroid moment tensor solutions in a heterogeneous earth: The CMT3D catalogue, *Geophys. J. Int.* **231,** no. 3, 1727–1738, doi: 10.1093/gji/ggac280.

Schorlemmer, D., and J. Woessner (2008). Probability of detecting an earthquake, *Bull. Seismol. Soc. Am.* **98,** no. 5, 2103–2117, doi: 10.1785/0120070105.

Schorlemmer, D., F. Mele, and W. Marzocchi (2010). A completeness analysis of the National Seismic Network of Italy, *J. Geophys. Res.* **115,** no. B4, doi: 10.1029/2008JB006097.

Schorlemmer, D., S. Wiemer, and M. Wyss (2005). Variations in earthquake-size distribution across different stress regimes, *Nature* **437,** no. 7058, 539–542, doi: 10.1038/nature04094.

Scordilis, E. M. (2006). Empirical global relations converting M_S and m_b to moment magnitude, *J. Seismol.* **10,** no. 2, 225–236, doi: 10.1007/s10950-006-9012-4.

Serra, I., and Á. Corral (2017). Deviation from power law of the global seismic moment distribution, *Sci. Rep.* **7,** no. 1, 40045, doi: 10.1038/srep40045.

Taroni, M., and J. Selva (2021). A testable worldwide earthquake faulting mechanism model, *Seismol. Res. Lett.* **92,** no. 6, 3577–3585, doi: 10.1785/0220200445.

Taroni, M., J. D. Zechar, and W. Marzocchi (2014). Assessing annual global M 6+ seismicity forecasts, *Geophys. J. Int.* **196,** no. 1, 422–431, doi: 10.1093/gji/ggt369.

Vavryčuk, V. (2015). Moment tensor decompositions revisited, *J. Seismol.* **19,** no. 1, 231–252, doi: 10.1007/s10950-014-9463-y.

Wessel, P. (2024). The origins of the Generic Mapping Tools: From table tennis to geoscience, *Perspect. Earth Space Sci.* **5,** no. 1, e2023CN000231, doi: 10.1029/2023CN000231.

Wessel, P., J. F. Luis, L. Uieda, R. Scharroo, F. Wobbe, W. H. F. Smith, and D. Tian (2019). The Generic Mapping Tools version 6, *Geochem. Geophys. Geosys.* **20,** no. 11, 5556–5564, doi: 10.1029/2019GC008515.

Wiemer, S., and M. Wyss (2000). Minimum magnitude of completeness in earthquake catalogs: Examples from Alaska, the western United States, and Japan, *Bull. Seismol. Soc. Am.* **90,** no. 4, 859–869, doi: 10.1785/0119990114.

Wimpenny, S., and C. S. Watson (2021). gWFM: A global catalog of moderate-magnitude earthquakes studied using teleseismic body waves, *Seismol. Res. Lett.* **92,** no. 1, 212–226, doi: 10.1785/0220200218.

Woessner, J., and S. Wiemer (2005). Assessing the quality of earthquake catalogues: Estimating the magnitude of completeness and its uncertainty, *Bull. Seismol. Soc. Am.* **95,** no. 2, 684–698, doi: 10.1785/0120040007.

Woodhouse, J. H., and A. M. Dziewonski (1984). Mapping the upper mantle: Three-dimensional modeling of Earth structure by inversion of seismic waveforms, *J. Geophys. Res.* **89,** no. B7, 5953–5986, doi: 10.1029/JB089iB07p05953.

Yoder, M. R., J. R. Holliday, D. L. Turcotte, and J. B. Rundle (2012). A geometric frequency–magnitude scaling transition: Measuring b= 1.5 for large earthquakes, *Tectonophysics* **532–535,** 167–174, doi: 10.1016/j.tecto.2012.01.034.

Zaccagnino, D., and C. Doglioni (2022). The impact of faulting complexity and type on earthquake rupture dynamics, *Commun. Earth Environ.* **3,** no. 1, 258, doi: 10.1038/s43247-022-00593-5.

Manuscript received 28 June 2024
Published online 11 October 2024